J Mater Sci (2007) 42:5508–5515
DOI 10.1007/s10853-006-1024-5

Study on structure and performance of polycarbonate urethane synthesized via different copolymerization methods

Jintang Guo · Meihua Zhao · Yan Ti · Bo Wang

Received: 3 June 2006 / Accepted: 25 September 2006 / Published online: 3 April 2007

Abstract Polycarbonate urethane (PCU) was synthesized using polycarbonate diol (PCN), 1, 4-butanediol (BD), and 4,4′-methylene bis(phenyl isocyanate) (MDI) as starting materials by both the melting one-shot method and the solution pre-copolymerization method, respectively. It was then characterized by Fourier transfer infrared spectroscopy (FT-IR), tensile test, thermogravimetric analysis (TGA), differential scanning calorimetry (DSC) and small-angle X-ray scattering (SAXS). The results show that the tensile strength increases as the content of the hard segment increases. The decomposition upon heating was observed in two stages i.e. decompositions of hard and soft segments. There is an obvious soft–hard glass transition temperature area, which proves the existence of the micro-phase separation structure. The micro-separation phenomenon becomes more obvious as the content of the hard segment increases. The maximal distance of the hard segment microdomain is estimated to be 2.932 nm from SAXS results. The PCU synthesized via the solution pre-copolymerization method has better mechanical performance and microphase separation structure.

Introduction

Polyurethanes are widely used in modern medical treatment due to its excellent mechanical properties and bio-compatibility. It can be used in a diverse range of implantable medical devices, such as blood-contact materials, heart valves, small diameter vascular grafts, insulators for pacemaker and blood pumps [1–3]. Implants have to be made by high bio-stable materials since they are required to remain in vivo for a long period. Though most of the polyurethanes have been proved to have many excellent properties, they are easy to degrade in vivo by hydrolyzing or oxidizing in the body [1, 4–6]. The polyester PU is prone to hydrolytic degradation in the body, while the polyether PU has better anti-hydrolytic performance but may undergo oxidative degradation in several ways [7–10]. More recently, considerable attentions have been paid to polycarbonate urethanes (PCUs) for their improved the mechanical performances compared to the traditional polyurethanes and for better properties in anti-hydrolyzation and anti-oxidation [11–13]. However, there is rarely any detailed report on the synthesis and characterization of PCU.

In 1990's, Gunatillake et al. [14] prepared a series of PCUs using poly(hexamethylene carbonate) diol, poly(decane carbonate) diol, poly(2,2-diethyl-1,3-propane carbonate) diol and poly(1,3-bis(4-hydroxybutyl)-1,1,3, 3-tetramethydisiloxane carbonate) as soft segments. The polyurethane based on poly(1,3-bis(4-hydroxybutyl)-1,1,3,3-tetramethydisiloxane carbonate) shows a good phase-separated morphology, with sharp hard segment melting endotherms and soft segment glass transitions close to that of the pure soft segment. The recent PCU syntheses mostly use poly(ethylene ether carbonate)diols [15], poly(hexamethylene carbonate)diol [14, 16], poly(tetramethylene carbonate)diol [16], poly(hexamethylene-co-pentamethylene carbonate)diol [16] and poly(-hexyl ethyl)carbonate diols [17] as soft segments. Xie et al. [16] synthesized a series of PCUs with different soft segments by the melting two-shot method. However, the

J. Guo (✉) · M. Zhao · Y. Ti · B. Wang
Department of Polymer Science and Engineering, School of Chemical Engineering and Technology, Tianjin University, Tianjin 300072, P.R. China
e-mail: jtguo@tju.edu.cn

studies on the micro-phase structure were insufficient. In this paper, PCU was prepared by the melting one-shot method and the solution pre-copolymerization method, and characterized by IR, DSC, TGA, SAXS, etc. The effects of different PCU composition and copolymerization methods on the micro-phase structure were also discussed. The micro-domain distance of the material was calculated according to the SAXS results.

Experimental

Materials

Polycarbonate diol(PCN, M_w = 1000, 1500, 2000, Beijing Santomer Chemical Co., Ltd.) was dried for 24 h at 80 °C under vacuum prior to use; 4,4′-methylenediphenyl diisocyanate (MDI, Mitsui Chemicals) and 1,4-butanediol(BD, imported) were distilled at reduced pressure before use; *N,N*-Dimethylacetamide (DMAC, Tianjin Ruijinte Chemicals Co.) was distilled from calcium hydride to ensure dryness; Tetrahydrofuran (THF, Tianjin University Kewei Co.) was dried by distiollation over sodium prior to use; Methanol (Tianjin University Kewei Co.) used was of HPLC-grade quality; Dibutyltin dilaurate (Tianjin Ruijinte Chemicals Co.) was used without further purification.

Melting one-shot method

PCN, BD and MDI were accurately weighted and melted in the beakers. The melted solution was then poured into a polytetrafluoroethylene stirring beaker. The temperature was controlled between 100–140 °C. The solution was vigorously stirred for 30 sec, and then poured onto a polytetrafluoroethylene board. The board was then placed in an oven of nitrogen atmosphere at 110 °C for 8 h.

Solution pre-copolymerization method

PCN and MDI were accurately weighted and prepared as 20% (w/v) DMAC solution. The solution was then poured into a four neck flask with nitrogen conduit tube. When the temperature rose to 75 °C and became stable, the catalyst, 0.1 wt% dibutyltin dilaurate, was added into the flask by drops. Allow it to react for some time, the 20% (w/v) BD solution in DMAC was added to the flask. The reaction continued for several hours before heating was stopped while leaving the stirring process for a while. The reaction was finally terminated by methanol. The above product was precipitated in the mixture solvent of ether and water. The final product was precipitated from water, washed by distilled water, placed statically at room temperature for 24 h, and vacuum dried at 50 °C for 72 h.

Measurements

Fourier transfer infrared spectroscopy (FT-IR)

The BIO-RAD FTS3000 FT-IR spectrometer was used to perform the FT-IR measurement with the testing range from 500–3500cm^{-1}. The PCU was quenched by liquid nitrogen, grinded into powder and coated on a KBr plate. Each spectrum was collected by accumulating 16 scans at a resolution of 0.25 cm^{-1} with DTGS as detector.

Tensile tests

The Testometric M350-10KN materials testing machine was used for tensile tests at test speed of 10 mm/min. The samples were pressed to make films at 170 °C by the machine and cut by a standard sample knife. The sample sheets had a width of 6.5 mm and thickness of 0.5 mm, with three samples for each compound.

Thermogravimetric (TG) analysis

The thermal stability of the material was characterized by the Shimadzu TG-50 thermogravimeter. The sample was heated from room temperature to 600 °C with a heating rate of 10 °C/min under the nitrogen atmosphere at the gas flow rate of 20 cm^3/min. The measurements were conducted using 6–10 mg samples. Weight-loss versus temperature curves were recorded.

Differential scanning calorimetry (DSC) analysis

The glass transition temperature was determined by the Shimadzu DSC-50 Differential Scanning Calorimeter under the nitrogen atmosphere at the gas flow rate of 20 cm^3/min. The temperature increased at the rate of 10 °C/min in the range of –80–250°C.

Small-angle X-ray scattering (SAXS) analysis

The X-ray patterns of samples were obtained by using the Riguka D/MAX 2500V/PC X-ray scatter with Cu Kα (λ = 0.154056 nm) radiation at 40 kV and 200 mA. The step size was 0.01 for 4 s from 0.1 to 10°.

Results and discussions

PCNs with three different molecular weights were selected and two different copolymerization methods were used to synthesize the PCUs in this paper, as shown in Table 1. Where, in PCUM10-121, M represents the melting

one-shot method, 10 means the molecular weight of the PCN is 1000, and 121 is the molar ratio of the raw materials, i.e. PCN, MDI and BD. In PCUA10-121, A represents the solution pre-copolymerization method.

Effects of synthesis methods on the properties of PCUs

FT-IR analysis

One sample was selected for the FTIR test from each synthesis method, and their spectra were shown in Fig. 1. It shows that the final products from each synthesis method are basically the same material. There is no stretch vibration peak of the NH at 3640 cm^{-1} in the FTIR spectra, while at 3323 cm^{-1}, there is a vibration peak of the NH joined with hydrogen bond. It indicates that all the NH in the hard segments participate the formation of the hydrogen bond. The peaks at 2940 cm^{-1} and 2855 cm^{-1} correspond to the CH_2 anti-symmetry and symmetry stretch vibration peaks in the soft segment of the PCN. The strong peak at 1741 cm^{-1} corresponds to the free C=O bond of the aliphatic carbonate. The peak at 1698 cm^{-1} belongs to C=O joined with the hydrogen bond in the urethane; 1597 cm^{-1} peak is the C=C bond vibration in the benzene; The strong and sharp peak at 1530 cm^{-1} is the joint frequency of the symmetry bent vibration of N–H bond and stretch vibration of the C=N. 1471 cm^{-1} peak is the symmetry bent vibration of the CH_2; 1243 cm^{-1} peak is the anti-symmetry vibration of the O–C = O in the soft segment of the PCN; 1067 cm^{-1} peak is the stretch vibration of the C–O–C of the urethane; 957 cm^{-1} peak is the symmetry stretch vibration of the C–O–C of the carbonate; 790 cm^{-1} peak corresponds to outside bent vibration zone of the adjacent hydrogen bonds on the aryl, which indicates there is a para-disubstituted benzene in the final product.

Mechanical properties of PCUs

The comparison of mechanical property between different synthetic methods was presented in Fig. 2. It shows that the PCUA has higher tensile strength. This is mainly due to the homogeneous distribution of the rigid and flexible chains in the material prepared by the solution pre-copolymerization. The better orderly accumulation helps to form the complete micro-phase separation.

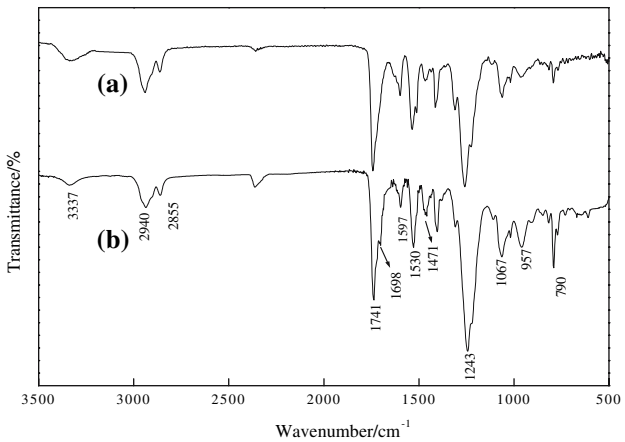

Fig. 1 FT-IR spectra of PCU, (**a**) PCUM15-132, (**b**) PCUA15-132

TG analysis of PCUs

Four samples were selected to perform the thermal analyses to investigate the thermal stability of the PCUs. The weight loss data were listed in Table 2. It is shown in Table 2 that there are two weight losses for all the PCU samples, which indicates that the decomposition of the PCU is a two-step reaction. It is concluded by a previous reference [18] that the first step of the PCU thermal decomposition is the simple depolymerization of urethane bonds, and the second step is the soft segment decomposition.

Figure 3 displays the DTG comparison between PCUs synthesized by the solution pre-copolymerization method (PCUA15-132) and the melting one-shot method (PCUM15-132). The pre-copolymerization method is relatively mild, which allows the complete stretch of the PCN

Table 1 Formula of PCUs

Samples	Appearance of PCUs	Samples	Appearance of PCUs	Content of hard segment (%)
PCUM10-132	White, hard	PCUA10-132	Yellow, hard	48.2
PCUM10-121	White, elastomeric	PCUA10-121	Yellow, elastomeric	37.1
PCUM10-231	White, elastomeric	PCUA10-231	Yellow, elastomeric	29.6
PCUM15-132	Yellow, elastomeric	PCUA15-132	Yellow, elastomeric	38.3
PCUM15-121	White, elastomeric	PCUA15-121	Yellow, elastomeric	28.2
PCUM15-231	Yellow, elastomeric	PCUA15-231	Yellow, elastomeric	21.9
PCUM20-132	White, hard	PCUA20-132	Yellow, elastomeric	31.7
PCUM20-121	White, elastomeric	PCUA20-121	Yellow, soft, incompact	22.8
PCUM20-231	Yellowy, hard	PCUA20-231	Yellow, soft, incompact	17.4

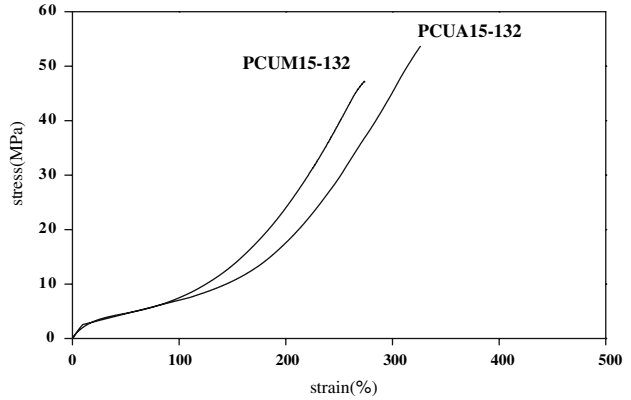

Fig. 2 Stress–strain curves of PCUs prepared by different synthesized methods, but with same raw materials ratio and soft segment molecular weight

long chain segment. The reaction has high stability and yields ordered accumulation of the chains and complete separation of micro phases. There are no overlapped peaks for the materials prepared by the solution pre-copolymerization method, which indicates the separation is more complete. If the two peaks represent the two steps of the thermal decomposition, the separation extent of the peaks indicates the separation of the two phases.

DSC analysis of PCUs

Seven samples were selected for the DSC measurement and the results were listed in Table 3. It is shown in Table 3 that there is an obvious glass transition temperature for all the prepared copolymers. The first one is the glass transition temperature of the soft segment T_{g1}, which is in the range of –40 °C to –20 °C. The second is the glass transition temperature of the hard segment T_{g2}, which is above 0 °C. The existence of two glass transition temperatures indicates the existence of the two separated phase structure. It is reported that the pure hard segment copolymer has a glass transition temperature between 90–100 °C [19]. The glass transition temperatures for these

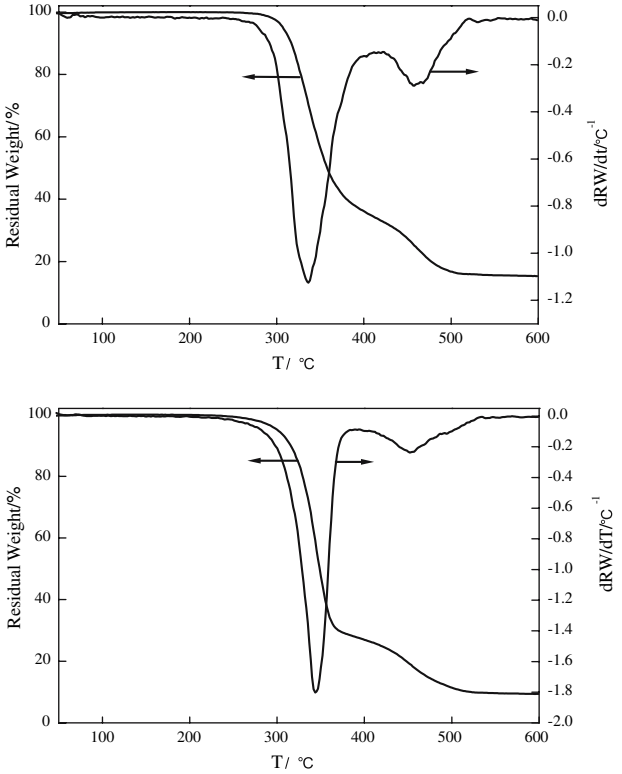

Fig. 3 TG and DTG curves of PCUs (Top: PCUM15-132; Bottom: PCUA15-132 Left: TG curves; Right: DTG curves)

samples are all below that of the pure copolymer. It indicates that the two phases have certain compatibility.

The comparisons between PCUM15-231 and PCUA15-231, PCUM20-132 and PCUA20-132 show that the differences of the glass transition temperatures between soft and hard segments are larger for the compounds prepared by the solution pre-copolymerization method. It indicates that the pre-copolymerization method yields a more completely separated micro phase product. This agrees with the results of TGA and the stress–strain test.

As shown in Table 3, an endotherm peak is observed at the intermediate temperature (T_m, 100–150 °C). It is possibly associated with the onset of the microphase

Table 2 TGA data of PCU

Sample	Content of hard segment (%)	Interval of weight loss (°C)	Weight loss (%)	Temperature of initial weight loss (°C)	Temperature of maximal rate of weight loss (°C)
PCUM15-121	28.2	50–432	80.1	269	352
		432–600	15.6	432	462
PCUM10-132	48.2	50–410	67.4	264	325
		410–600	21	410	458
PCUM15-132	38.3	50–413	66	260	337
		413–600	19.7	413	460
PCUA15-132	38.3	50–387	71.9	247	343
		387–600	18.9	387	453

Table 3 DSC data of PCU

Sample	Tg1 (onset, midpoint, end) (°C)			Tg2 (onset, midpoint, end) (°C)			Endotherm peak (°C)
PCUM10-132	–13	–11	8	83	86	89	170
PCUM15-231	–30	–17	–9	39	47	55	116
PCUM15-121	–24	–16	–7	69	76	81	148
PCUM20-132	–35	–26	–18	47	51	55	127
PCUA15-231	–38	–27	–18	48	53	59	108
PCUA15-132	–41	–32	–19	71	79	88	153
PCUA20-132	–41	–35	–29	47	54	63	141

separation transition process (MST) [20]. The apparent MST temperatures are found to increase with the increasing in hard-segment content. T_m for the PCUs prepared by the melting one-shot method and the solution pre-copolymerization method are almost the same.

Effects of raw materials ratio

Mechanical properties of PCUMs

Figure 4 shows the stress–strain curves of the PCUM prepared with the soft segment molecular weight of 1500. The mechanical curves of PCUM prepared by the 1000 and 2000 soft segment molecular weight are similar to this. It can be observed from Fig. 4 that the tensile strength of the PCU increases as the hard segment content increases and the fracture strain decreases at the same time. The elastic long chain molecules in the PCU may usually curl irregularly. However, due to the inner-molecular and intermolecular bonding, quenching, or other outside forces, the elastic chains of the PCU are forced to form ordered array. The chains can hardly move or rotate, which results in the crystallization of chains. When the hard segment content is small, it cannot form the relatively independent micro domain and has to disperse into the soft segments, which destroys the crystallization of the soft segment. This results in the decreasing of the tensile strength of the material. The elastic material is then a compatible system. With the increasing of the hard segment content, a certain amount of the hard segment phases begins to accumulate and form the micro domain. At the same time, some crystals may be formed and they increase the separation extent of the micro-phase in the elastomer. The crystallization possibility of the soft segment is improved after the micro-phase separation, which increases the tensile strength of the PCU.

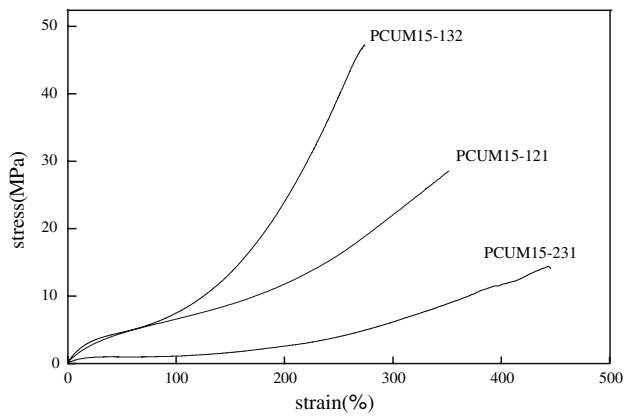

Fig. 4 Stress–strain curves of PCUs with different raw materials ratio, but prepared by same synthesized method and soft segment molecular weight 1500; the curves of PCUM prepared by 1000 and 2000 area

TG analysis of PCUMs

Since the content of isocyanate in PCUM15-132 is higher than that in the PCUM15-121 and the reaction time of the melting one-shot method is short, for the first decomposition step, there was possible formation of the urea-formate by the reaction of partial NCO with adjacent urethane bonds. The thermal stability of the above group had been investigated with the result that its thermal decomposition stability is the worst among all the groups obtained from the isocyanate reacted with different kinds of the active hydrogen [21]. Hence, the initial weight loss temperature and the highest weight loss rate temperature decrease as the hard segment content increases (as shown in Table 2). The bond energy of the C–O is higher than that of the C–N, the soft segment is therefore not easy to be broken. With different content of the hard segment, less hard segment means less C–N bond and more C–O bond in the main chain. Therefore, the initial weight loss temperature and the highest weight loss rate temperature of the second step increase as the hard segment content decreases.

DSC analysis of PCUMs

The comparison between PCUM15-231 and PCUM15-121, as shown in Table 3, indicates that when the soft segment molecular weight is the same, T_{g1} is rarely changed but T_{g2} is obviously increased as the hard segment content in the

copolymer increases. This is possibly due to the high soft segment content of these samples. Changes of the soft segment content have insignificant effect on the glass transition temperature. However, when the hard segment content increases, it causes the glass transition temperature to increase dramatically due to the formation of the relative independent micro domain of the hard segment or even the crystallization. The larger difference of the two glass transition temperatures indicates the larger separation of the two phases. Hence, with the same soft segment molecular weight, the higher hard segment content results in the higher separation extent of the two phases.

Effects of soft segment molecular weight

Mechanical properties of PCUMs

Figure 5 presents that the tensile strength of the PCUM is the highest when using the PCN with the molecular weight of 2000. The possible reasons are as follows. First of all, with the increase of the PCN molecular weight, the amount of ester and methylene increases, which increases both the Van der Waals forces and the hydrogen bond forces. At the same time, the increase of the molecular chain length will easily form folding chains, which makes the crystallization of the soft segments easier. The tensile strength of the material increases when the soft segment has higher crystallinity. The material may be of necking phenomenon, which results in the increasing of the strain. Secondly, the longer soft segment molecular chain makes the permeation of the hard segment into the soft segment difficult. The micro-phase separation extent is then higher in the PCU. The existence of the micro domain helps to distribute the stress and improve the tensile strength.

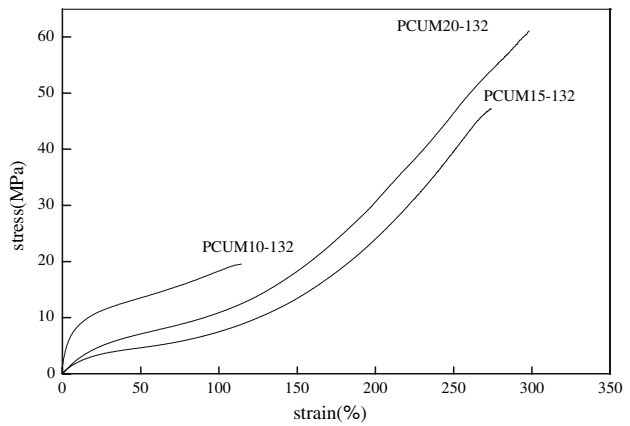

Fig. 5 Stress–strain curves of PCUs with different soft segment molecular weight, but prepared by same synthesized method and raw materials ratio

TG analysis of PCUMs

The increase of the soft segment molecular weight lengthens the distance between the hard segment micro domain and reduces the hydrogen bond formation ability between the hard segments, which decreases the initial weight loss temperature in the first step. At the same time, the increase of the soft segment molecular weight makes the soft segment micro domain well arranging, which results in the ordered micro domains and makes crystallization easier, so that the initial weight loss temperature in the second step is enhanced. The effect of the soft segment molecular weight is the competitive result of the above two roles. It is found from Table 2 that the effect of increasing the soft segment molecular weight on the weight loss temperature is negligible. However, the highest weight loss rate temperature increased 12 °C for the first step.

DSC analysis of PCUMs

Comparison between PCUM10-132 and PCUM20-132 from Table 3 shows that the glass transition temperatures are both obviously changed. When the raw material molar ratio is the same, the hard segment glass transition temperature T_{g2} decreases as the soft segment molecular weight increases. The reason for this possibly is that on the one hand, the increase of the soft segment molecular weight destroys the tropistic effect between the soft and hard segment, which makes the accumulation of the hard segment into the ordered micro domain difficult and the hard segment scattered in the soft segment; on the other hand, it also destroys the huge amount of hydrogen bonds in the PCU and boosts the mixing of the two phase areas, which decreases the hard segment glass transition temperature T_{g2}, the decomposition entropy as well as the phase separation extent of the hard and soft segments.

SAXS analysis of PCUs

In order to estimate the maximal distance of the hard segment micro-domain, three samples were selected for the analysis, i.e. PCUM15-121, PCUM15-231 and PCUM20-231. Generally, 2θ is the scattering angle in the X-ray scattering, λ is the incoming wave length and I is the wave intensity, s and S are angle coefficients. The above coefficients have the following relationships: $s = 2\sin\theta/\lambda \approx 2\theta/\lambda$, $S = 2\pi s \approx 4\pi\theta/\lambda$. Since the scattering angle exists at the small angle region, we took the approximation, that is, $\sin\theta \approx \theta$. The SAXS of PCUM15-121 is shown in Fig. 6.

It is shown in Fig. 6 that there are scattering peaks at $S = 0.55\ nm^{-1}$ and $2.63\ nm^{-1}$. According to the inverse-proportional law for all the scattering phenomena of the electromagnetic wave, the larger the materials dimension,

the smaller the scattering angel as far as the wave length is concerned. It is also because that there is the crystallization melting peak for the hard segment but not for the soft segment in the DSC, therefore the scattering peak at 0.55 nm^{-1} possibly is the peak of the PCU hard segment micro domain. And the scattering peak at 2.63 nm^{-1} probably is from the hard segment crystalline domain.

The curve shape showed in Fig. 6 is a typical SAXS plot of the copolymer. If we assume the system has uniform particle size and shape, the following equation can be used in calculation:

$$I(s) = I(0)\exp\left(-\frac{4}{3}\pi^2 s^2 R\right) \quad (3.1)$$

where R is the cyclotron radius in the system. Take ln of Eq. 3.1, yielding

$$\ln I(S) = \ln I(0) - \frac{1}{3}R^2S^2 \quad (3.2)$$

The above equation shows that the plot of S^2 vs. lnI(S) is a linear line in a certain range with the intercept of lnI(0) and the slope of $1/3R^2$. There are two phases in the PCU structure, hence there should be two linear regions. The replot of the SAXS curves yields two linear plots with the linear fitting equations of Y = 7.55898–100.61405X and Y = 7.745–18.21902X(showed in Fig 7). The cyclotron radius of the hard segment micro domain R_1 and the cyclotron radius of the crystalline domain R_2 can then be obtained. The radii of the hard segment micro domain and crystalline domain can also be calculated from $R^2 = (3/5)r^2$, and the hard segment micro domain distance can be estimated from $d_{max} = 2.44\pi/S_{max}$[22].

The results from these three samples are shown in Table 4.

It is shown in Table 4 that the radius and distance of the hard segment micro domain both increase as the hard segment content decreases. While the hard segment crystalline domain radius decrease and the distance increases with insignificant changes in total, which indicates that the crystallinity of the hard segment decreases as its content decreases. PCU is a two-phase material with alternative soft and hard segments. The distance between soft segments and that between hard segments should be the same. Hence, the material has micro phase separation structure [23].

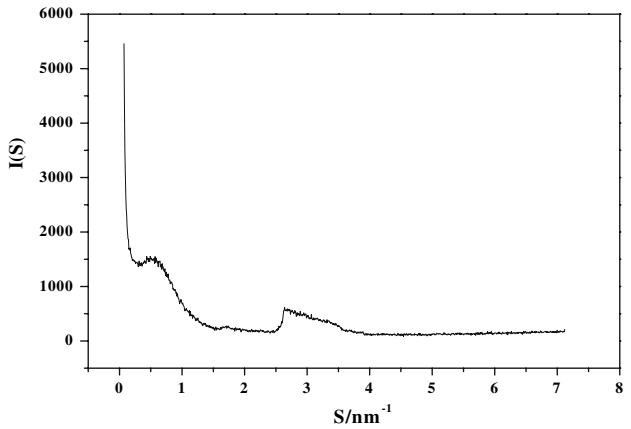

Fig. 6 SAXS curve of PCUM15-121

Conclusions

PCU with the soft segment PCN molecular weight of 1000, 1500, and 2000, were synthesized by melting one-shot method and solution pre-copolymerization method, respectively. The FTIR measurement shows that the products from the above two methods have the same PCU structure.

The tensile test shows that the tensile strength increases but the fracture strain decreases as the hard segment content increases. TG analyses shows that there are two steps of the thermal decomposition of PCU. The changes in

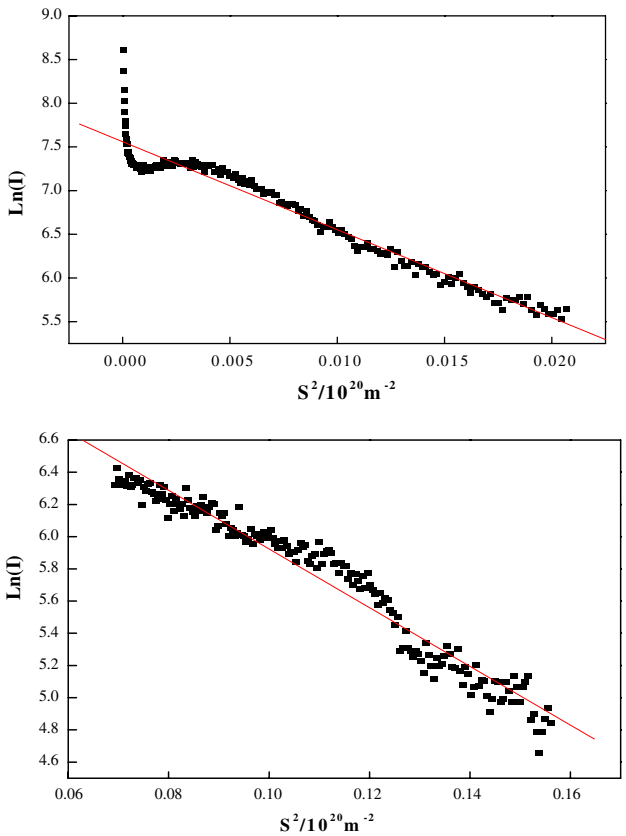

Fig. 7 Linear fit curves of Ln(S)-S2. Top: linear fit curve of hard segment micro domain; Bottom: linear fit curve of hard segment crystallization domain

Table 4 SAXS data analysis of PCU

Sample	Content of hard segment (%)	R_1 (nm)	r_1 (nm)	d_1 (nm)	R_2 (nm)	r_2 (nm)	d_2 (nm)
PCUM15-121	28.2	1.737	2.242	13.9	0.739	0.954	2.826
PCUM15-231	21.9	1.916	2.474	16.0	0.731	0.944	2.872
PCUM20-231	17.4	2.271	2.932	22.9	0.724	0.935	2.880

copolymerization method, raw materials ratio and the soft segment molecular weight all influence the thermal decomposition temperature. DSC shows obvious glass transition area of the soft and hard segments. The two glass transition temperatures are in between temperatures for the pure hard segment and soft segment glass transition. SAXS analyses yields the radii of the hard segment micro domain and the crystallization domain, cyclotron radius, and distance between micro domains. These tests proved the separation of the two phases of PCU.

References

1. Pinchuk L (1994) J Biomater Sci Polym Ed 6(3):225
2. Thomas V, Kumari TV, Jayabalan M (2001) Biomacromolecules 2(2):588
3. Capone CD (1992) J Biomater Appl 7(2):108
4. Anderson JM, Hiltner A, Wiggins MJ, Schuber MA, Collier TO, Kao WJ, Matheur AB (1998) Polym Int 46(3):163
5. Stokes K, McVenes R, Anderson JM (1995) J Biomater Appl 9(4):321
6. Howard GT (2002) Int Biodeterior Biodegrad 49(4):245
7. Takahara A, Coury AJ, Hergenrother RW, Cooper SL (1991) J Biomed Mater Res 25(3):341
8. Wiggins MJ, Wilkoff B, Anderson JM, Hiltner A (2001) J Biomed Mater Res 58(3):302
9. Zhao Q, Agger MP, Fitzpatrick M, Anderson JM, Hiltner A, Stokes K, Urbanski P (1990) J Biomed Mater Res 24(5):621
10. Zhao Q, Topham N, Anderson JM, Hiltner A, Lodoen G, Payet CR (1991) J Biomed Mater Res 25(2):177
11. Khan I, Smith N, Jones E, Finch DS, Cameron RE (2005) Biomaterials 26(6):621
12. Khan I, Smith N, Jones E, Finch DS, Cameron RE (2005) Biomaterials 26(6):633
13. Tanzi MC, Mantovani D, Petrini P, Guidoin R, Laroche G (1997) J Biomed Mater Res 36(4):550
14. Gunatillake PA, Meijs GF, Mccarthy SJ, Adhikari R, Sherriff N (1998) J Appl Polym Sci 69(8):1621
15. Harris RF, Joseph MD, Davidson C, Deporter CD, Dais VA (1990) J Appl Polym Sci 41(3):487
16. Xie XY, Li JH, Zhong YP, He CS, Fan CR (2002) Polym Mater Sci Eng 18(6):37
17. Hsu SH, Lin ZC (2004) Colloid Surf B 36(1):1
18. Fu XS, Chen F, Li HP, Wei YP (2005) Chem Ind Eng 22(4):267
19. Brunette CM, Hsu SL, Macknight WJ (1982) Macromolecules 15(1):71
20. Leung LM, Koberstein JT (1998) Macromolecules 19(3):706
21. Colodny PC, Tobolsky AV (1957) J Am Chem Soc 79(16):4320
22. Yu H, Wang J, Natansohn A, Singh MA (1999) Macromolecules 32(13):4365
23. Chang SL, Yu TL, Huang CC, Chen WC, Liu KL, Lin TL (1998) Polymer 39(15):3479